4-15-2015

Identification of a negative regulatory role for Spi-C in the murine B cell lineage

Stephen K.H. Li
Western University

Lauren A. Solomon
Western University

Patricia C. Fulkerson
Cincinnati Children's Hospital Medical Center

Rodney P. De Koter
Western University, rdekoter@schulich.uwo.ca

The Journal of Immunology

Identification of a Negative Regulatory Role for Spi-C in the Murine B Cell Lineage

Stephen K. H. Li, Lauren A. Solomon, Patricia C. Fulkerson and Rodney P. DeKoter

J Immunol 2015; 194:3798-3807; Prepublished online 13 March 2015;
doi: 10.4049/jimmunol.1402432
http://www.jimmunol.org/content/194/8/3798

The Journal of Immunology is published twice each month by
The American Association of Immunologists, Inc.,
1451 Rockville Pike, Suite 650, Rockville, MD 20852

Print ISSN: 0022-1767 Online ISSN: 1550-6606.

Identification of a Negative Regulatory Role for Spi-C in the Murine B Cell Lineage

Stephen K. H. Li,*,† Lauren A. Solomon,*,† Patricia C. Fulkerson,‡ and Rodney P. DeKoter*,†

Spi-C is an E26 transformation-specific family transcription factor that is highly related to PU.1 and Spi-B. Spi-C is expressed in developing B cells, but its function in B cell development and function is not well characterized. To determine whether Spi-C functions as a negative regulator of Spi-B (encoded by *Spib*), mice were generated that were germline knockout for *Spib* and heterozygous for *Spic* (*Spib*$^{-/-}$*Spic*$^{+/-}$). Interestingly, loss of one *Spic* allele substantially rescued B cell frequencies and absolute numbers in *Spib*$^{-/-}$ mouse spleens. *Spib*$^{-/-}$*Spic*$^{+/-}$ B cells had restored proliferation compared with *Spib*$^{-/-}$ B cells in response to anti-IgM or LPS stimulation. Investigation of a potential mechanism for the *Spib*$^{-/-}$*Spic*$^{+/-}$ phenotype revealed that steady-state levels of *Nfkb1,* encoding p50, were elevated in *Spib*$^{-/-}$*Spic*$^{+/-}$ B cells compared with *Spib*$^{-/-}$ B cells. Spi-B was shown to directly activate the *Nfkb1* gene, whereas Spi-C was shown to repress this gene. These results indicate a novel role for Spi-C as a negative regulator of B cell development and function. ***The Journal of Immunology*****, 2015, 194: 3798–3807.**

B cell development occurs in the bone marrow of mammals, where committed progenitor B (pro-B) cells are generated from lymphoid progenitor cells. Pro-B cells develop into mature B cells through a series of defined stages marked by rearrangement of Ig H and L chain genes. Immature B cells leaving the bone marrow are termed transitional type 1 (T1) B cells, which migrate to the spleen and differentiate into transitional type 2 (T2) B cells (1). T2 B cells can mature into either follicular (FO) or marginal zone (MZ) B cells that go on to participate in Ab formation and immune regulation (1).

Transcription factors function as either activators or repressors of gene expression to govern B cell development. E26 transformation-specific (ETS) transcription factors PU.1 (encoded by *Spi1*) and Spi-B (encoded by *Spib*) function as transcriptional activators during B cell development. PU.1 is required to generate B cell progenitors, because *Spi1*$^{-/-}$ mice have a profound block in B cell development (2, 3). *Spib*$^{-/-}$ mice have reduced numbers of B cells that are defective in BCR signaling and are unable to sustain Ab responses to T-dependent Ags (4, 5). PU.1 and Spi-B activate transcription by interacting with the consensus core motif 5′-GGAA-3′ at specific sites within the genome (6). As a result of the similarities in DNA-binding specificities and overlapping expression patterns, many gene targets are functionally redundant between PU.1 and Spi-B, although there are also exclusive roles for each (4, 7, 8).

Transcriptional networks that control B cell differentiation include both transcriptional activators and repressors (9). Interestingly, few published examples of negative regulators of ETS transcription factor function exist. Spi-C is an ETS transcription factor that is a potential negative regulator. Spi-C was originally described as a PU.1-related protein containing an N-terminal acid-activation domain (10–12). Ectopic overexpression of Spi-C in either cultured pro-B cells using a retroviral vector (13) or in mice using a B cell–specific transgene (Eμ–Spi-C) (14) suggested that Spi-C functions as a negative regulator by opposing PU.1 activity. Transgenic Spi-C expression under the control of the B cell–specific *IgH* intronic enhancer resulted in reduced absolute numbers of T1, T2, MZ, and FO B cells in Eμ–Spi-C mice compared with wild-type (WT) mice (14). Recently a *Spic*-knockout mouse was generated, allowing for Spi-C loss-of-function analysis (15). Spi-C was revealed to be essential for generating red pulp macrophages in the spleen and is inducible by Heme (16). Spi-C is upregulated in Bach1/Bach2-knockout B cells and results in altered gene expression patterns in B cells (17). Therefore, Spi-C may have a regulatory role in B cells for development and function.

The goal of this study was to determine whether Spi-C plays a negative regulatory role in B cell development and function. A loss-of-function approach was used by crossing a *Spic*-null allele onto a *Spib*-knockout background (*Spib*$^{-/-}$*Spic*$^{+/-}$ mice). The effect of *Spic* heterozygosity in *Spib*$^{-/-}$ mice might have no effect on the phenotype, further impair B cell development, or rescue the *Spib*$^{-/-}$ phenotype. It was observed that *Spic* heterozygosity substantially rescued both the development and function of B cells in *Spib*$^{-/-}$ mice. Taken together, our results identify a negative regulatory role for Spi-C in B cells.

Materials and Methods

Generation and breeding of mice

Mice were housed at Western University's Health Sciences animal facility and monitored under an approved animal use subcommittee protocol in accord with Western University Council on Animal Care.

*Department of Microbiology and Immunology, Centre for Human Immunology, Schulich School of Medicine and Dentistry, Collaborative Graduate Program in Developmental Biology, Western University, London, Ontario N6A 5C1, Canada; †Division of Genetics and Development, Children's Health Research Institute, Lawson Research Institute, London, Ontario N6C 2V5, Canada; and ‡Division of Allergy and Immunology, Cincinnati Children's Hospital Medical Center, Cincinnati, OH 45229

Received for publication September 23, 2014. Accepted for publication February 9, 2015.

This work was supported by grants from the Canadian Institutes of Health Research (MOP-106581) and the National Sciences and Engineering Research Council (Grant 386046) (to R.P.D.). S.K.H.L. was the recipient of an Ontario Graduate Scholarship.

Address correspondence and reprint requests to Dr. Rodney P. DeKoter, Department of Microbiology and Immunology, Schulich School of Medicine and Dentistry, Western University, London, Ontario N6A 5C1, Canada. E-mail address: rdekoter@uwo.ca

The online version of this article contains supplemental material.

Abbreviations used in this article: ChIP, chromatin immunoprecipitation; ETS, E26 transformation specific; FO, follicular; MZ, marginal zone; pro-B, progenitor B; qPCR, quantitative PCR; T1, transitional type 1; T2, transitional type 2; T3, transitional type 3; TSS, transcription start site; WT, wild-type.

C57BL/6 (WT) mice were purchased from Charles River Laboratories (Pointe-Claire, QC, Canada). *Spib*$^{+/-}$*Spic*$^{+/-}$ mice were backcrossed to C57BL/6 mice for five generations prior to the generation of *Spib*$^{-/-}$*Spic*$^{+/-}$ mice. *Spib*$^{-/-}$*Spic*$^{+/-}$ mice were generated by crossing male and female *Spib*$^{-/-}$*Spic*$^{+/-}$ mice. Eμ–Spi-C *Spib*$^{-/-}$*Spic*$^{+/-}$ mice were generated by crossing Eμ–Spi-C^{+} male mice with *Spib*$^{-/-}$*Spic*$^{+/-}$ females. Genotyping was performed by PCR, as previously described (7, 15). All experiments were performed on mice aged 6–12 wk.

B cell enrichment and proliferation analysis

RBCs were removed from spleen cell suspensions by hypotonic lysis with ammonium chloride solution. B cells were enriched by negative selection using biotin-conjugated anti-CD43 (S7) Ab, streptavidin MicroBeads, LD depletion columns, and a QuadroMACS separation unit (Miltenyi Biotec, Bergisch Gladbach, Germany). B cells (2×10^5/well) were plated in 96-well flat-bottom plates and stimulated with LPS (10 μg/ml; List Biological Laboratories), anti-IgM Ab [50 μg/ml, affinity pure F(ab′)$_2$ fragment], or goat anti-mouse IgM Ab (μ chain specific; Jackson ImmunoResearch Laboratories) in complete IMDM. Proliferation was assessed after 72 h of incubation at 37°C with a TACS MTT Cell Proliferation assay (Trevigen, Gaithersburg, MD), according to the manufacturer's instructions. For CFSE analysis, 10×10^6 B cells were stained with 5 μM CFSE (BioLegend, San Diego, CA) for 5 min at room temperature prior to plating. Frequency of stained cells was assessed after 72 h of incubation at 37°C by flow cytometry.

Flow cytometry

Abs and reagents purchased from eBioscience (San Diego, CA), BD Bioscience (Franklin Lakes, NJ), or BioLegend included 7-amino-actinomycin D, CFSE, Brilliant Violet 421–conjugated anti-CD45R/B220 (Ra3-6B2), allophycocyanin-conjugated IgM (II/41), allophycocyanin-conjugated annexin V, biotin-conjugated anti-CD43 (S7), PE-conjugated CD93 (AA4.1), PE-conjugated anti–BP-1 (BP-1), PE-conjugated anti-CD19 (1D3), PE-conjugated phospho-Syk (moch1ct), FITC-conjugated CD24 (30-F1), FITC-conjugated anti-CD21/CD35 (eBio8D9), FITC-conjugated anti-CD23 (B3B4), and PE-Cy5–conjugated streptavidin. Cells were blocked with purified anti-CD16/CD32 (Mouse BD Fc Block). Intracellular staining was performed using a two-step protocol and an intracellular fixation and permeabilization buffer set obtained from eBioscience. Ab-stained cell analysis was performed using FACSCalibur and LSR II systems, and sorting was performed using a FACSAria III system (BD Biosciences). Sorted cells were determined to be >98% pure. Data analysis was performed using FlowJo software (TreeStar, Ashland, OR).

Reverse transcription–quantitative PCR

RNA was isolated with TRIzol reagent (Invitrogen, Burlington, ON, Canada). cDNA was synthesized using an iScript cDNA Synthesis Kit (Bio-Rad, Mississauga, ON, Canada), and quantitative PCR (qPCR) was performed with a Rotor-Gene 6000 instrument (Corbett Life Sciences, Valencia, CA). Relative mRNA transcript levels were normalized to β_2-microglobulin and compared between samples using the comparative threshold cycle method. Calculations were performed using REST 2009 software (18). Primer sequences are listed in Supplemental Table I.

Immunoblot analysis

Lysates were prepared using Laemmli buffer and applied to 8–10% SDS polyacrylamide gels for electrophoresis. Proteins were transferred to nitrocellulose membranes using a Trans-Blot Semi-Dry system (Bio-Rad), and membranes were blocked for 1 h in 5% milk in TBST. Membranes were probed with anti–Spi-C (Aviva Systems Biology, San Diego, CA), anti-Flag (M2; Sigma-Aldrich, St. Louis, MO), anti-Syk (C-20; Santa Cruz Biotechnology, Dallas, TX), or anti–β-actin (I-19; Santa Cruz Biotechnology) Ab and diluted to the manufacturers' recommended concentrations in 1% milk/TBST overnight at 4°C. A secondary HRP-conjugated anti-goat Ab was incubated in 1% milk/TBST. Membranes were washed and visualized with SuperSignal West Pico reagent (Thermo-Fisher Scientific).

ELISAs

Serum was collected and quantified for IgG2b and IgM. ELISA kits were purchased from eBioscience and performed according to the manufacturer's instructions. ELISA plates were analyzed using an Epoch microplate spectrophotometer with Gen5 software (BioTek, Winooski, VT).

Plasmids and cloning

Spi-C cDNA was cloned into the hemagglutinin tag-containing pcDNA3 vector, as previously described (13). The *Nfkb1* promoter was amplified from C57BL/6 genomic DNA by PCR using LA Taq (TaKaRa; Clontech Laboratories, Mountain View, CA), purified, and cloned into the pSC-A vector using a PCR cloning kit (Agilent Technologies, La Jolla, CA). A 468-bp *Nfkb1* promoter was PCR amplified using a forward primer containing a HindIII site and subcloned. The promoter was HindIII digested from pSC-A and ligated into the HindIII site of the pGL3-basic (Promega, Madison, WI) luciferase reporter vector. ETS binding sites were mutated using the QuikChange Lightning Site-Directed Mutagenesis Kit, according to the manufacturer's instructions (Agilent Technologies). Constructs were verified by DNA sequencing. Plasmid DNA was prepared by growth in DH5α bacteria and purified with a Maxi Plasmid Kit (Geneaid, New Taipei City, Taiwan). All restriction enzymes were purchased from New England Biolabs (Ipswich, MA). Primer sequences used for cloning are listed in Supplemental Table I.

Transient transfection

WEHI-279 MIGR1, MIG–3XFLAG–Spi-B, and MIG–3XFLAG–Spi-C cells were generated, as previously described (7, 19). Cells in mid to early log-phase growth were washed three times with serum-free DMEM (4.5 g/l; Wisent, St-Bruno, QC, Canada) and incubated for 10 min at room temperature with 10 μg each luciferase reporter plasmid and 1 μg pRL-TK (Promega). Cell–DNA mixtures were electroporated at 220 V and 950 mF using 4-mm gap cuvettes with a Gene Pulser II with Capacitance Extender (Bio-Rad), incubated at room temperature for 10 min, transferred to six-well culture plates in complete DMEM, and incubated at 37°C for 24 h. A Dual-Luciferase Reporter Assay System (Promega) was performed on cell lysates. Light production was measured using a Lumat LB 9507 tube luminometer (Berthold Technologies, Oak Ridge, TN).

Chromatin immunoprecipitation experiments

Chromatin was prepared from enriched B cells, as previously described (7, 19). Cells were cross-linked and lysed, followed by sonication. Sonicated chromatin was incubated overnight at 4°C with anti–Spi-C (generated by the Fulkerson laboratory) and anti-FLAG (M2; Sigma-Aldrich) conjugated to protein G Dynabeads (Invitrogen). Bead complexes were enriched using a MagneSphere Technology Magnetic Separation Stand (Promega) and washed. Immunocomplexes were eluted, and cross-links were reversed overnight at 65°C. DNA was purified using a QIAquick PCR Purification Kit (QIAGEN, Limburg, The Netherlands). Enrichment was measured using qPCR of immunoprecipitated DNA with the primers indicated in Supplemental Table I.

Statistical analysis

Statistical significance was determined using one-way or two-way ANOVA analysis, with a Bonferroni posttest, unless otherwise indicated. The p values ≤ 0.05 were considered significant. Statistical analyses were performed using Prism 5.0 (GraphPad).

Results

Restored splenic B cell numbers in Spib$^{-/-}$Spic$^{+/-}$ *mice compared with* Spib$^{-/-}$Spic$^{+/+}$ *mice*

To determine the roles of Spi-C in B cell development, mice homozygous for germline-null alleles of *Spib* (4) and heterozygous *Spic* (15) were mated. *Spib*$^{-/-}$*Spic*$^{+/-}$ mice were generated in Mendelian ratios (Table I) and were healthy and fertile. However, few *Spib*$^{-/-}$*Spic*$^{-/-}$ mice were generated (Table I). Therefore, these studies focused on analysis of *Spib*$^{-/-}$*Spic*$^{+/+}$ and *Spib*$^{-/-}$*Spic*$^{+/-}$ mice.

To determine that the haploid state of Spi-C is insufficient in *Spib*$^{-/-}$*Spic*$^{+/-}$ mice, immunoblot analysis was performed on WT, *Spib*$^{-/-}$, and *Spib*$^{-/-}$*Spic*$^{+/-}$ spleen lysates to detect protein levels of Spi-C. A reduction in Spi-C was measured in *Spib*$^{-/-}$*Spic*$^{+/-}$ spleen lysates compared with those from WT or *Spib*$^{-/-}$ mice (Fig. 1A). As previously noted, *Spib*$^{-/-}$ mice had reduced total numbers of splenocytes compared with WT mice (Fig. 1B). However, total numbers of splenocytes were substantially rescued in *Spib*$^{-/-}$*Spic*$^{+/-}$ mice compared with *Spib*$^{-/-}$ mice (Fig. 1B). To assess the population of mature B cells, frequencies of B220^{+}CD93^{-} cells were determined using flow cytometry (Fig. 1C). *Spib*$^{-/-}$ spleens contained decreased frequencies of mature B cells and decreased absolute numbers of mature B cells. In contrast, *Spib*$^{-/-}$*Spic*$^{+/-}$ spleens had substantially rescued frequencies and absolute numbers of

Table I. Expected and actual frequencies of mouse genotypes from offspring generated by mating male and female Spib$^{-/-}$Spic$^{+/-}$ mice

Genotype	No. of Mice Produced	Expected Frequency[a] (%)	Actual Frequency[b] (%)
Spib$^{-/-}$*Spic*$^{+/+}$	101	25	36.5
Spib$^{-/-}$Spic$^{+/-}$	174	50	62.8
Spib$^{-/-}$*Spic*$^{-/-}$	2	25	0.7

[a]Expected frequencies are based on Mendelian ratios.
[b]Actual frequencies are based on the genotyping of 277 pups.

mature B cells compared with *Spib*$^{-/-}$ spleens (Fig. 1D). Overall, these results showed that knocking out one allele of *Spic* on a *Spib*$^{-/-}$ background rescued absolute number of mature B cells in *Spib*$^{-/-}$ spleens. These results suggest that Spi-C levels are involved in regulating B cell differentiation.

Rescued absolute number of FO B cells in Spib$^{-/-}$Spic$^{+/-}$ *spleens compared with* Spib$^{-/-}$ *spleens*

Spib$^{-/-}$ mice were reported to have reduced frequencies of FO B cells (7). To determine whether mature B cell populations were restored in *Spib*$^{-/-}$*Spic*$^{+/-}$ spleens, flow cytometry was performed on splenocytes from WT, *Spib*$^{-/-}$, and *Spib*$^{-/-}$*Spic*$^{+/-}$ mice. Mature B cells were gated on B220^{+}CD93^{-}, followed by analysis of CD21 and IgM surface expression to identify FO (CD21^{low}IgM^{int}) and MZ (CD21^{high}IgM^{hi}) B cells (Fig. 1E). Absolute numbers of MZ B cells were unaffected by either reduced Spi-B or Spi-C expression. However, FO B cells were decreased in both frequency and absolute number in *Spib*$^{-/-}$ spleens compared with WT spleens (Fig. 1F). *Spib*$^{-/-}$*Spic*$^{+/-}$ spleens contained restored absolute numbers of FO B cells compared with *Spib*$^{-/-}$

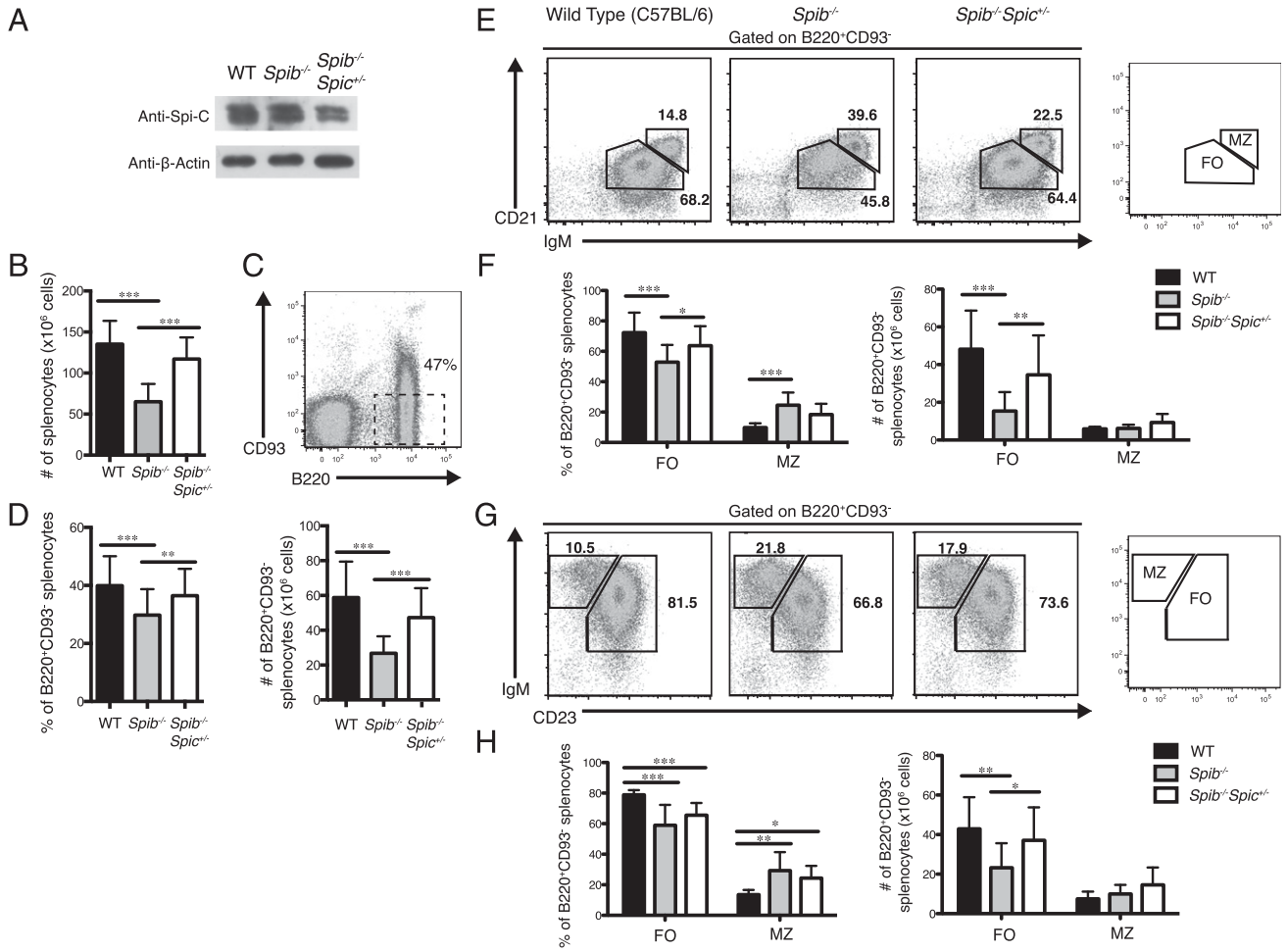

FIGURE 1. Spi-C heterozygosity rescues absolute numbers of FO B cells in the spleens of *Spib*$^{-/-}$ mice. (**A**) Spi-C protein expression measured in WT, *Spib*$^{-/-}$, and *Spib*$^{-/-}$*Spic*$^{+/-}$ spleen lysates. Immunoblot was performed using anti–Spi-C Ab and anti–β-actin as a loading control. Data shown are a representative of three individual experiments. (**B**) Cell counts based on total cells isolated from the spleens of WT, *Spib*$^{-/-}$, and *Spib*$^{-/-}$*Spic*$^{+/-}$ mice. (**C**) Mature B cells were quantified by flow cytometry based on B220 and CD93. The dashed box represents the mature B cell population. (**D**) Quantitation of the frequency and absolute number of B220^{+}CD93^{-} splenocytes identified in WT, *Spib*$^{-/-}$, and *Spib*$^{-/-}$*Spic*$^{+/-}$ mice. (**E**) Mature FO and MZ B cell populations were quantified based on CD21 and IgM surface expression. (**F**) Quantitation of the frequency and absolute number of MZ (CD21^{high}IgM^{high}) and FO (CD21^{low}IgM^{int}) mature B cells (B220^{+}CD93^{-}) in the spleen. (**G**) Mature FO and MZ B cell populations were quantified based on CD23 and IgM surface expression. Cells were isolated from WT, *Spib*$^{-/-}$, and *Spib*$^{-/-}$*Spic*$^{+/-}$ spleens and analyzed by flow cytometry. (**H**) Quantitation of the frequency and absolute number of MZ (CD23^{low}IgM^{high}) and FO (CD23^{high}IgM^{int}) mature B cells (B220^{+}CD93^{-}) in the spleen. Data in (B) and (D) are mean and SD of 14 individual mice; data in (F) and (H) are mean and SD of 9 individual mice. *$p < 0.05$, **$p < 0.01$, ***$p < 0.001$.

spleens (Fig. 1F). Next, MZ and FO B cell populations were quantified by CD23 and IgM surface expression (Fig. 1G). Absolute numbers of MZ B cells ($IgM^{high}CD23^{-/low}$) were unchanged among WT, *Spib*$^{-/-}$, and *Spib*$^{-/-}$*Spic*$^{+/-}$ spleens. However, frequencies of FO B cells ($IgM^{int}CD23^{+}$) were reduced in *Spib*$^{-/-}$ spleens, and this reduction was rescued in *Spib*$^{-/-}$*Spic*$^{+/-}$ spleens (Fig. 1H). Taken together, these results suggest that the rescue of the absolute numbers of mature B cells in *Spib*$^{-/-}$*Spic*$^{+/-}$ spleens was primarily a result of increased FO B cells.

Increased transitional B cells in Spib$^{-/-}$Spic$^{+/-}$ *spleens compared with* Spib$^{-/-}$ *spleens*

Because *Spib*$^{-/-}$*Spic*$^{+/-}$ spleens had increased numbers of FO B cells compared with *Spib*$^{-/-}$ spleens, it was hypothesized that there were increased immature B cells developing in the bone marrow of these mice. To test this, flow cytometry analysis was performed using the "Hardy" staining scheme for bone marrow cells (20) (Fig. 2A). Although *Spib*$^{-/-}$ mice had increased fraction D and reduced fraction F populations compared with WT B cells, no significant differences in the frequencies of fractions A through F were observed between *Spib*$^{-/-}$ and *Spib*$^{-/-}$*Spic*$^{+/-}$ mice (Fig. 2B, 2C). These results suggested that restored FO B cell numbers were not due to an increase in the frequency of B cell progenitors derived from the bone marrow.

To assess whether rates of apoptosis were altered in *Spib*$^{-/-}$*Spic*$^{+/-}$ B cells, flow cytometry was performed on WT, *Spib*$^{-/-}$, and *Spib*$^{-/-}$*Spic*$^{+/-}$ spleens. Cells were gated into T1, T2, MZ, and FO B cell populations based on B220, CD93, IgM, and CD23 staining, and apoptotic cells were gated for Annexin V^{+}7-AAD^{-} (Supplemental Fig. 1A). No differences were detected in apoptotic frequency in total B cells (Supplemental Fig. 1B) or gated T1, T2, MZ, or FO B cells (Supplemental Fig. 1C) among WT, *Spib*$^{-/-}$, and *Spib*$^{-/-}$*Spic*$^{+/-}$ mice. These results suggest that reduced Spi-C expression does not significantly alter steady-state levels of apoptosis in *Spib*$^{-/-}$ mice.

To determine the source of rescued numbers of FO B cells in *Spib*$^{-/-}$*Spic*$^{+/-}$ spleens compared with *Spib*$^{-/-}$ spleens, immature transitional B cell populations were examined. Immature B cells were gated on expression of both B220 and CD93 (Fig. 3A). There were increased frequencies of $B220^{+}CD93^{+}$ immature B cells in both *Spib*$^{-/-}$ and *Spib*$^{-/-}$*Spic*$^{+/-}$ spleens compared with WT spleens, but there was no significant difference in the frequency of these cells between *Spib*$^{-/-}$ and *Spib*$^{-/-}$*Spic*$^{+/-}$ spleens. In contrast, absolute numbers of immature B cells were nearly doubled in *Spib*$^{-/-}$*Spic*$^{+/-}$ spleens compared with WT or *Spib*$^{-/-}$ spleens (Fig. 3B). To determine which immature B cell subset was accountable for overall increased numbers, analysis of T1, T2, and transitional type 3 (T3) B cell populations was performed by gating immature $B220^{+}CD93^{+}$ B cells for differential expression of IgM and CD23 (Fig. 3C). No differences in T3 B cells were observed among WT, *Spib*$^{-/-}$, and *Spib*$^{-/-}$*Spic*$^{+/-}$ spleens. In contrast, *Spib*$^{-/-}$ and *Spib*$^{-/-}$ *Spic*$^{+/-}$ spleens contained elevated frequencies and absolute numbers of T1 B cells compared with WT spleens, although there was no quantitative difference in the T1 population between *Spib*$^{-/-}$ and *Spib*$^{-/-}$*Spic*$^{+/-}$ mice. For T2 populations, *Spib*$^{-/-}$ spleens contained fewer cells than did WT spleens, and both the frequency and absolute numbers of T2 cells were rescued in *Spib*$^{-/-}$*Spic*$^{+/-}$ spleens (Fig. 3D). To confirm that T2 B cell numbers were rescued in *Spib*$^{-/-}$*Spic*$^{+/-}$ spleens compared with *Spib*$^{-/-}$ spleens, splenic B cells were examined using an alternative staining scheme based on CD21 and IgM expression (Supplemental Fig. 2A). Absolute numbers of T2 B cells were significantly reduced in *Spib*$^{-/-}$ spleens compared with WT spleens and were rescued in *Spib*$^{-/-}$*Spic*$^{+/-}$ spleens using the alternative staining scheme (Supplemental Fig. 2B). In summary, these results showed that reduced Spi-C in *Spib*$^{-/-}$*Spic*$^{+/-}$ mice resulted in a substantial rescue of the frequency of T2 cells in the spleen of *Spib*$^{-/-}$ mice.

LPS- and anti-IgM–mediated proliferation is rescued in Spib$^{-/-}$Spic$^{+/-}$ *B cells compared with* Spib$^{-/-}$ *B cells*

B cells lacking Spi-B were reported to have impaired proliferative responses to either LPS or anti-IgM (4, 5). To determine whether *Spic* heterozygosity could rescue functional defects in *Spib*-knockout B cells, proliferation of *Spib*$^{-/-}$ and *Spib*$^{-/-}$*Spic*$^{+/-}$ splenic B cells in response to LPS or anti-IgM was assessed using an MTT proliferation assay. Compared with WT B cells, *Spib*$^{-/-}$ B cells proliferated poorly in response to LPS or anti-IgM (Fig. 4A). In contrast, *Spib*$^{-/-}$*Spic*$^{+/-}$ B cells were substantially rescued for LPS- or anti-IgM–mediated proliferation compared with *Spib*$^{-/-}$ B cells (Fig. 4A, 4B). To confirm the proliferation rescue, LPS-mediated proliferation was measured by flow cytometry following the staining B cells with CFSE (Fig. 4C). Fewer cells underwent cell division in *Spib*$^{-/-}$ B cells stimulated with LPS compared with WT B cells. However, more proliferating cells were detected in *Spib*$^{-/-}$*Spic*$^{+/-}$ B cells compared with *Spib*$^{-/-}$ B cells (Fig. 4D). Therefore, these results suggest that B cell proliferation in response to LPS or anti-IgM is positively regulated by Spi-B but is negatively regulated by Spi-C.

To determine whether the *Spib*$^{-/-}$*Spic*$^{+/-}$ B cell phenotype could be reversed by ectopic expression of Spi-C, *Spib*$^{-/-}$*Spic*$^{+/-}$ mice were crossed to Eμ–Spi-C–transgenic mice (14). Spleens from Eμ–Spi-C *Spib*$^{-/-}$*Spic*$^{+/-}$ mice contained fewer cells than did *Spib*$^{-/-}$*Spic*$^{+/-}$ spleens (Fig. 4E). Flow cytometry analysis was performed on Eμ–Spi-C *Spib*$^{-/-}$*Spic*$^{+/-}$ spleens to assess for differences in B cell populations. Frequencies of MZ and FO B cells in Eμ–Spi-C *Spib*$^{-/-}$*Spic*$^{+/-}$ spleens were unchanged compared with *Spib*$^{-/-}$*Spic*$^{+/-}$ spleens; however, there was a significant reduction in the absolute number of MZ and FO B cells in Eμ–Spi-C *Spib*$^{-/-}$*Spic*$^{+/-}$ mice (Fig. 4F). Proliferation of Eμ–Spi-C*Spib*$^{-/-}$*Spic*$^{+/-}$ B cells following LPS stimulation was assessed by CFSE staining. Compared with *Spib*$^{-/-}$*Spic*$^{+/-}$ B cells, frequencies of proliferating Eμ–Spi-C*Spib*$^{-/-}$*Spic*$^{+/-}$ B cells decreased (Fig. 4G). These data suggest that reintroducing Spi-C using a lymphocyte-specific transgene reverses the *Spib*$^{-/-}$*Spic*$^{+/-}$ B cell–proliferation phenotype.

Because anti-IgM–mediated proliferation was restored in *Spib*$^{-/-}$*Spic*$^{+/-}$ B cells compared with *Spib*$^{-/-}$ B cells, it was possible that *Spib*$^{-/-}$*Spic*$^{+/-}$ B cells could have restored BCR signaling. To test for this, phosphorylated levels of Syk were measured in B cells using flow cytometry (Fig. 4H). There was a detectable increase in phospho-Syk levels following anti-IgM stimulation; however, there was no difference in the increase among WT, *Spib*$^{-/-}$, and *Spib*$^{-/-}$*Spic*$^{+/-}$ B cells (Fig. 4I). Next, total Syk was measured in B cells using immunoblot analysis. There was a noticeable increase in total Syk protein in *Spib*$^{-/-}$ and *Spib*$^{-/-}$*Spic*$^{+/-}$ B cells compared with WT B cells (Fig. 4J). Therefore, the restoration of BCR signaling in *Spib*$^{-/-}$*Spic*$^{+/-}$ B cells is likely downstream of Syk.

It was reported previously that *Spib*$^{-/-}$ mice had normal basal levels of all Ig isotypes (4). To determine whether reduced Spi-C had an effect on isotype switching in *Spib*$^{-/-}$*Spic*$^{+/-}$ mice, basal serum levels of different Igs were measured by ELISA. No significant differences in basal levels of IgM (Supplemental Fig. 3A) or IgG2b (Supplemental Fig. 3B) were measured among WT, *Spib*$^{-/-}$, and *Spib*$^{-/-}$*Spic*$^{+/-}$ mice. Therefore, the data suggest that Spi-C does not alter basal levels of Ig isotypes in *Spib*$^{-/-}$*Spic*$^{+/-}$ mice.

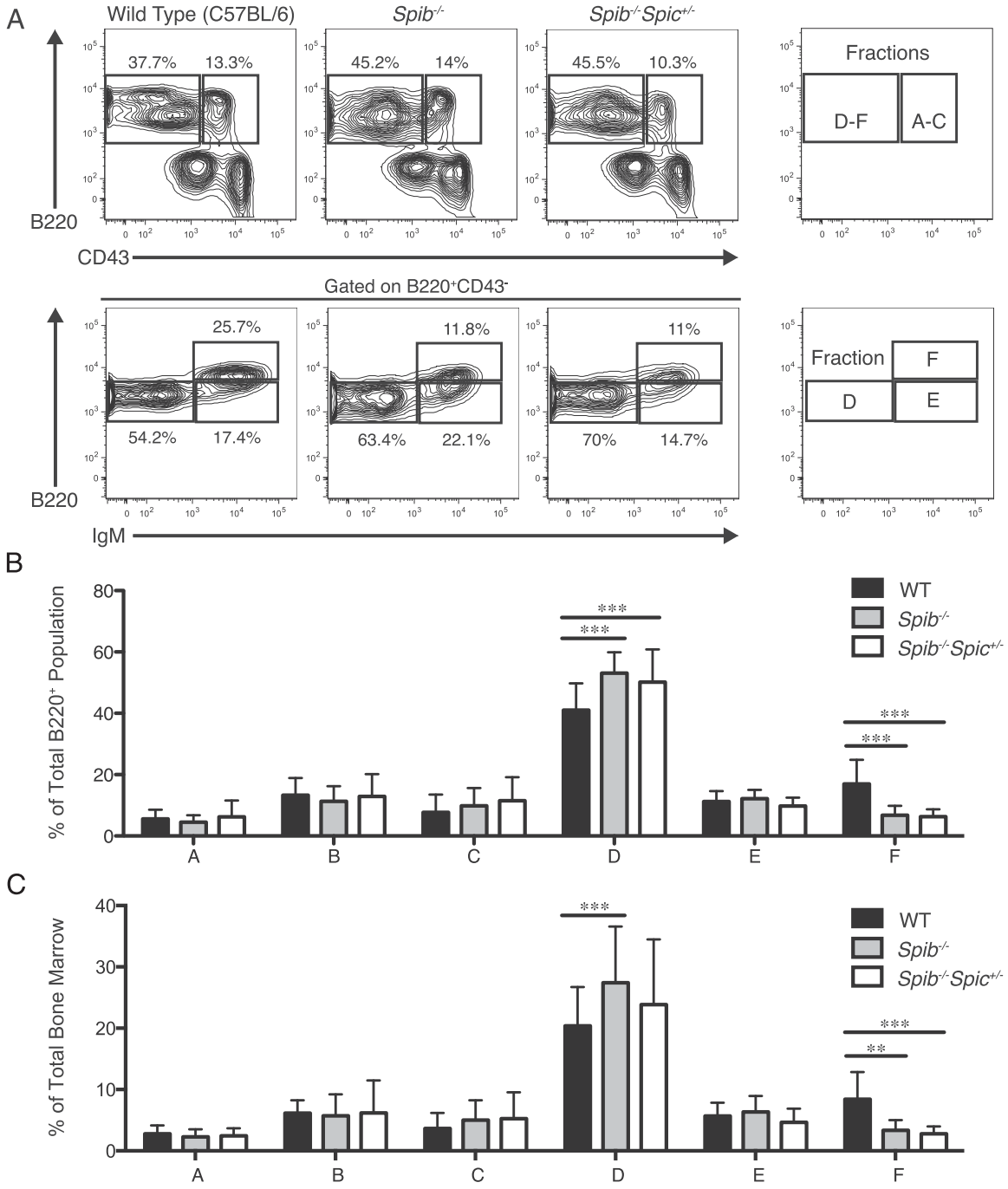

FIGURE 2. No differences in B cell composition between *Spib*$^{-/-}$ and *Spib*$^{-/-}$*Spic*$^{+/-}$ mice in the bone marrow. (**A**) Bone marrow analysis was performed on WT, *Spib*$^{-/-}$, and *Spib*$^{-/-}$*Spic*$^{+/-}$ mice. Cells were analyzed by flow cytometry and gated using the Hardy scheme for quantifying B cell populations during development. Data shown are a representative of eight individual mice. (**B**) Quantitation of individual fractions A–F located in the bone marrow calculated as a percentage of total B220^{+} cells in the bone marrow. (**C**) Quantitation of individual fractions A–F located in the bone marrow calculated as a percentage of total cells in the bone marrow. Fractions were gated using the Hardy scheme. Data in (B) are mean and SD of eight individual mice. $^{**}p < 0.01$, $^{***}p < 0.001$.

Spi-C represses Nfkb1 *promoter activation by Spi-B*

Finally, a potential mechanism for Spi-C's regulation of B cell proliferation was investigated. Stimulation of B cells with LPS or anti-IgM results in NF-κB transcription factor activation (21). P50 (encoded by *Nfkb1*) is required for murine B cell proliferation in response to LPS or anti-IgM (22). We recently showed that PU.1 and Spi-B are required for *Nfkb1* transcription in B cells, and retroviral transduction with p50 substantially rescues LPS-induced proliferation of *Spi1*$^{+/-}$*Spib*$^{-/-}$ B cells (23). Therefore, it was determined whether restored proliferation in *Spib*$^{-/-}$*Spic*$^{+/-}$ B cells was associated with increased mRNA transcript levels of *Nfkb1* compared with *Spib*$^{-/-}$ B cells. Reverse transcription–qPCR was performed on cDNA synthesized from MZ and FO B cells sorted from *Spib*$^{-/-}$ and *Spib*$^{-/-}$*Spic*$^{+/-}$ spleens. Steady-state *Nfkb1* mRNA transcript levels were increased in MZ and FO B cells from *Spib*$^{-/-}$*Spic*$^{+/-}$ mice compared with *Spib*$^{-/-}$ mice (Fig. 5A), suggesting that Spi-C may negatively regulate *Nfkb1* in B cells.

To assess whether Spi-B and Spi-C regulate *Nfkb1* directly, the murine *Nfkb1* promoter sequence was aligned with multiple species using a published transcription start site (TSS) for reference (24). The *Nfkb1* 5′ untranslated region contained two highly

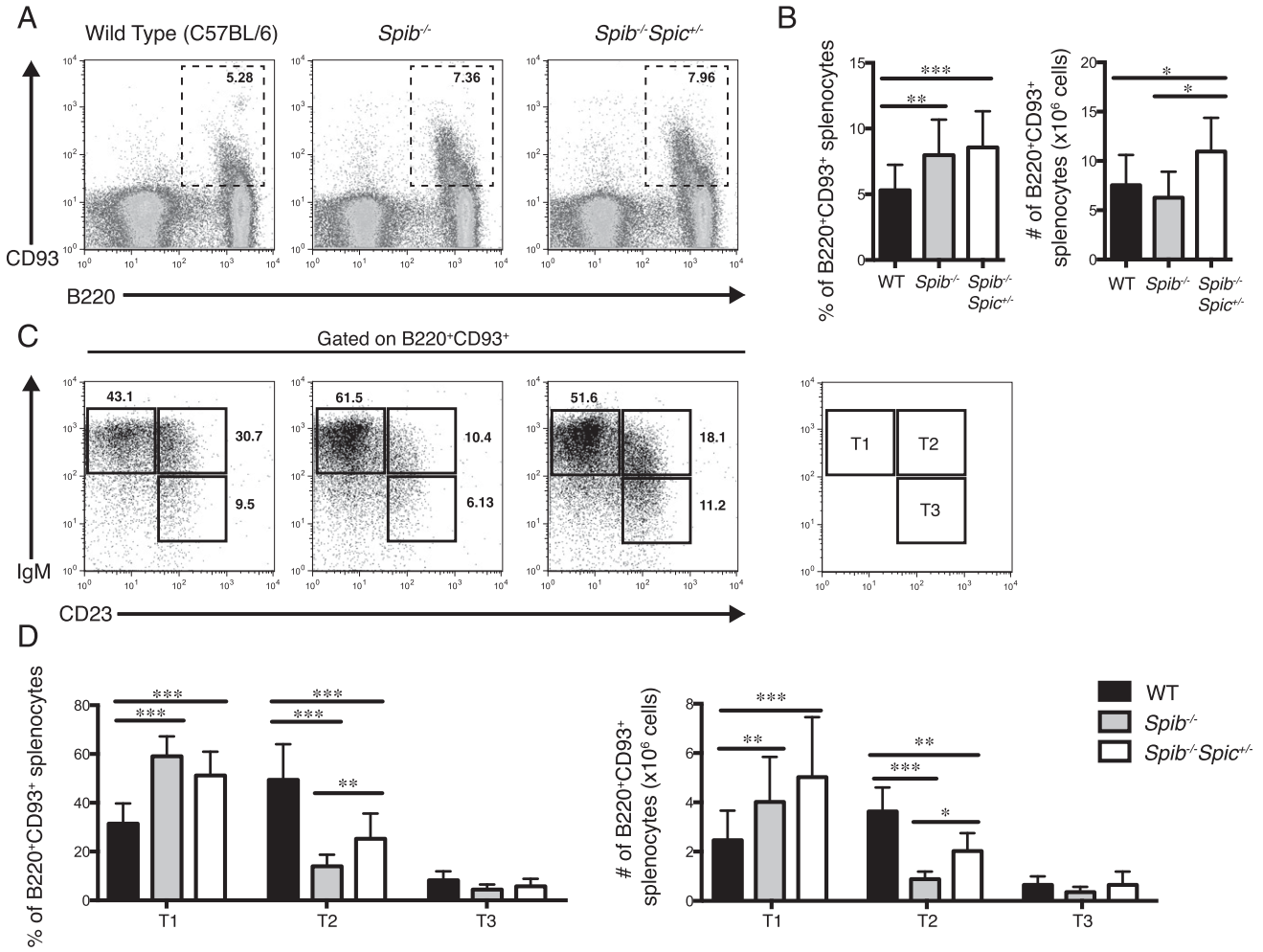

FIGURE 3. *Spib*$^{-/-}$*Spic*$^{+/-}$ mice have elevated transitional B cells and restored T2 B cells compared with *Spib*$^{-/-}$ mice. (**A**) Total transitional B cell populations were quantified in WT, *Spib*$^{-/-}$, and *Spib*$^{-/-}$*Spic*$^{+/-}$ mice. The dashed box represents total transitional B cells. Splenocytes were stained with CD93 and B220 and analyzed by flow cytometry. (**B**) Increased frequencies and absolute number of total transitional B cells in spleens of *Spib*$^{-/-}$ and *Spib*$^{-/-}$*Spic*$^{+/-}$ mice. (**C**) Transitional B cell subsets T1 (upper left quadrant, IgM^{high}CD23^{-}), T2 (upper right quadrant, IgM^{high}CD23^{+}), and T3 (lower right quadrant, IgM^{low} CD23^{+}) were quantified in WT, *Spib*$^{-/-}$, and *Spib*$^{-/-}$*Spic*$^{+/-}$ mice. Cells were gated on B220 and CD93 and analyzed for IgM and CD23 staining by flow cytometry. (**D**) Restored T2 subset in *Spib*$^{-/-}$*Spic*$^{+/-}$ mice compared with *Spib*$^{-/-}$ mice. Quantitation of results shown in (C). Data are mean frequency and absolute numbers of gated B220^{+}CD93^{+} splenocytes. Data in (B) and (D) are mean and SD of nine individual mice. *$p < 0.05$, **$p < 0.01$, ***$p < 0.001$.

conserved ETS binding sites predicted among all species near the TSS using MatInspector software (Fig. 5B). Next, the mouse *Nfkb1* proximal promoter was cloned, as described in *Materials and Methods*, and ligated into the pGL3-basic luciferase reporter vector. Site-directed mutagenesis was performed to mutate two predicted ETS binding sites closest to the TSS by substituting GGAA (TTCC on complement strand) with GGAC (GTCC), which was reported previously to abolish Spi-B binding (7, 19) (Fig. 5C). To determine whether Spi-B and Spi-C regulate *Nfkb1* transcription in opposing fashion, luciferase assays were performed using transient transfection of WEHI-279 B lymphoma cells that ectopically express 3XFLAG-tagged Spi-B or Spi-C (7, 19). WEHI-279 cells infected with an empty MIGR1 virus were used as a control (WEHI-279 MIGR1). Expression of 3XFLAG Spi-B and Spi-C protein was confirmed by anti-FLAG immunoblot analysis in infected cell lines (Fig. 5D). The *Nfkb1* promoter was active in WEHI-279 MIGR1 cells, and mutation of the ETS sites impaired its activation (Fig. 5E). WEHI-279 Spi-B cells displayed a higher level of activation compared with WEHI-279 MIGR1 cells, whereas mutation of the ETS sites reduced *Nfkb1* activation. Interestingly, the activity of the *Nfkb1* promoter in WEHI-279 Spi-C cells was lower than in both WEHI-279 MIGR1 and WEHI-279 Spi-B cells, and mutation of the ETS site resulted in no change of activity (Fig. 5E). To confirm that Spi-C expression decreased *Nfkb1* transcriptional activation, luciferase activity was measured following cotransfection of a Spi-C expression vector (pcDNA3 Spi-C) and the pGL3-*Nfkb1* vector into WEHI-279 Spi-B cells. Cotransfection with pcDNA3 Spi-C resulted in decreased *Nfkb1* activation compared with cotransfection with the vector control (pcDNA3) (Fig. 5F). These results suggest that Spi-B transcriptionally activates *Nfkb1*, and Spi-C inhibits *Nfkb1* transcription.

We recently showed that PU.1 and Spi-B directly interact with the *Nfkb1* promoter to activate its transcription (23). To determine whether Spi-C directly interacts with the *Nfkb1* promoter, chromatin immunoprecipitation (ChIP) analysis was performed using anti–Spi-C and anti-FLAG Ab on chromatin isolated from WEHI-279 Spi-C and WEHI-279 MIGR1 cells. Relative amounts of immunoprecipitated DNA were determined by qPCR from the *Nfkb1* promoter region, as well as the *Gapdh* promoter as a negative control. ChIP analysis confirmed that Spi-C was significantly enriched at the *Nfkb1* promoter compared with the *Gapdh* promoter in WEHI-279 Spi-C cells but not in WEHI-279 MIGR1 cells (Fig. 5G). Together, these data indicate that Spi-C directly

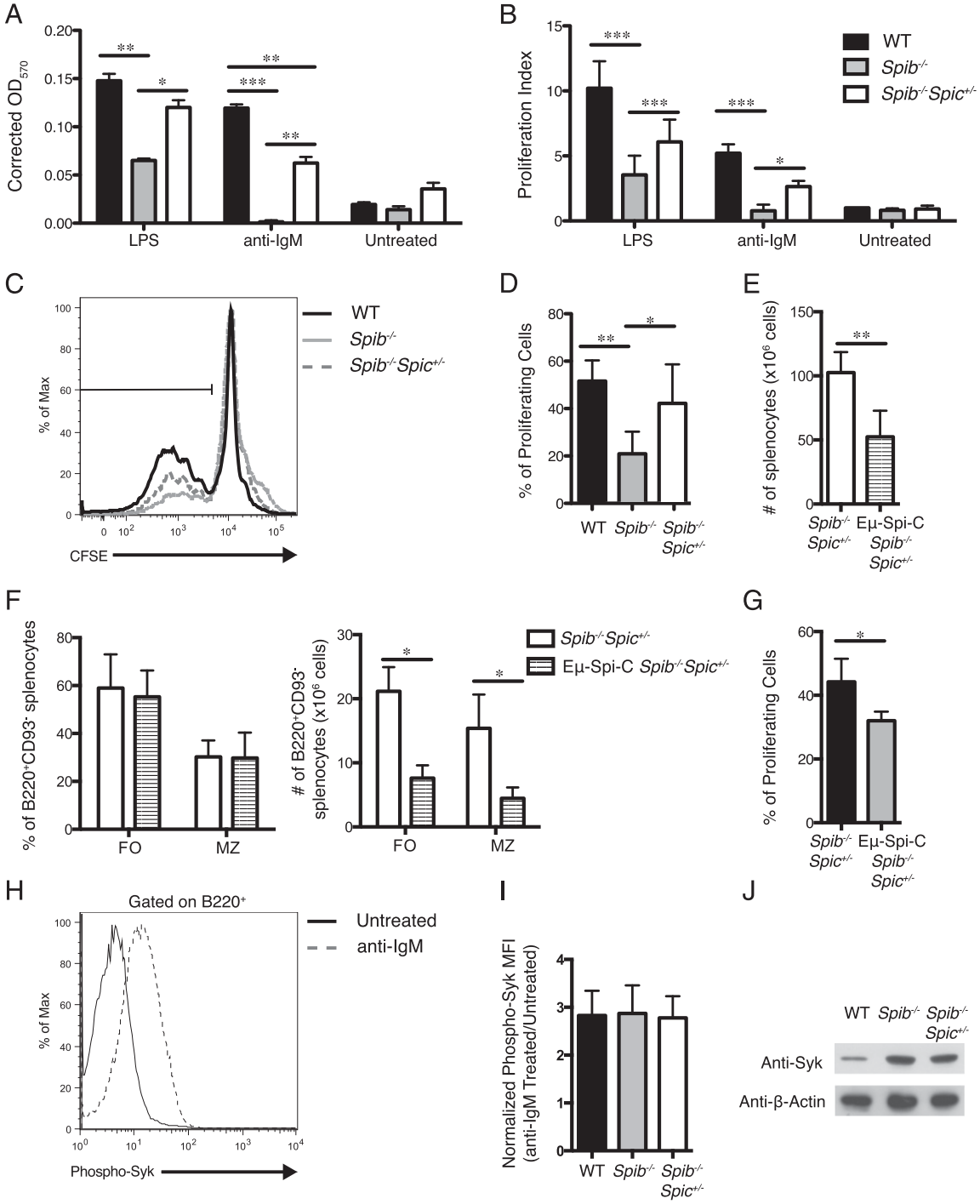

FIGURE 4. B cell proliferation is rescued in *Spib*$^{-/-}$*Spic*$^{+/-}$ mice compared with *Spib*$^{-/-}$ mice. (**A**) *Spib*$^{-/-}$*Spic*$^{+/-}$ B cells have a rescue in proliferation compared with *Spib*$^{-/-}$ B cells. Proliferation was measured using an MTT proliferation assay. Data are mean and SD of triplicate wells and are a representative of five experiments. (**B**) Quantitation of five experiments from (A) showing proliferation index, which was calculated by normalizing corrected OD_{570} values to the untreated WT control. Data are mean and SEM. (**C**) Proliferation assessed by flow cytometry following CFSE staining on WT, *Spib*$^{-/-}$, and *Spib*$^{-/-}$*Spic*$^{+/-}$ B cells. Gate shown represents the frequency of proliferating cells. Data shown are a representative of four individual experiments. (**D**) Quantitation of CFSE experiments, as performed in (C), showing frequency of cells that underwent cell division. (**E**) Cell counts based on total cells isolated from the spleens of *Spib*$^{-/-}$*Spic*$^{+/-}$ and Eμ–Spi-C *Spib*$^{-/-}$*Spic*$^{+/-}$ mice. (**F**) Quantitation of the frequency and absolute number of MZ and FO mature B cells ($B220^+CD93^-$) in the spleens of *Spib*$^{-/-}$*Spic*$^{+/-}$ and Eμ–Spi-C *Spib*$^{-/-}$*Spic*$^{+/-}$ mice. FO and MZ B cell populations were quantified based on CD23 and IgM surface expression measured by flow cytometry. Data in (E) and (F) are mean and SD of five individual mice. (**G**) Proliferation assessed by flow cytometry following CFSE staining on *Spib*$^{-/-}$*Spic*$^{+/-}$ and Eμ–Spi-C *Spib*$^{-/-}$*Spic*$^{+/-}$ B cells. Data are mean and SD for four individual experiments. (**H**) Phospho-Syk levels were assessed in WT, *Spib*$^{-/-}$, and *Spib*$^{-/-}$*Spic*$^{+/-}$ B cells using flow cytometry. Splenocytes were stained with B220, stimulated with anti-IgM for 2 min or left untreated, and stained with phospho-Syk prior to analysis. (**I**) Quantitation of phospho-Syk levels in $B220^+$ splenocytes following anti-IgM stimulation. Phospho-Syk levels are shown as normalized phospho-Syk mean fluorescence intensity (MFI) of anti-IgM to untreated. Data are mean and SD of five individual experiments. (**J**) Syk protein expression measured in WT, *Spib*$^{-/-}$, and *Spib*$^{-/-}$*Spic*$^{+/-}$ B cell lysates. Immunoblot was performed using anti-Syk Ab and anti–β-actin as a loading control. Data are a representative of three individual experiments. For (A)–(D) and (G), total B cells were enriched by magnetic separation and stimulated with LPS or anti-IgM for 72 h. $*p < 0.05$, $**p < 0.01$, $***p < 0.001$.

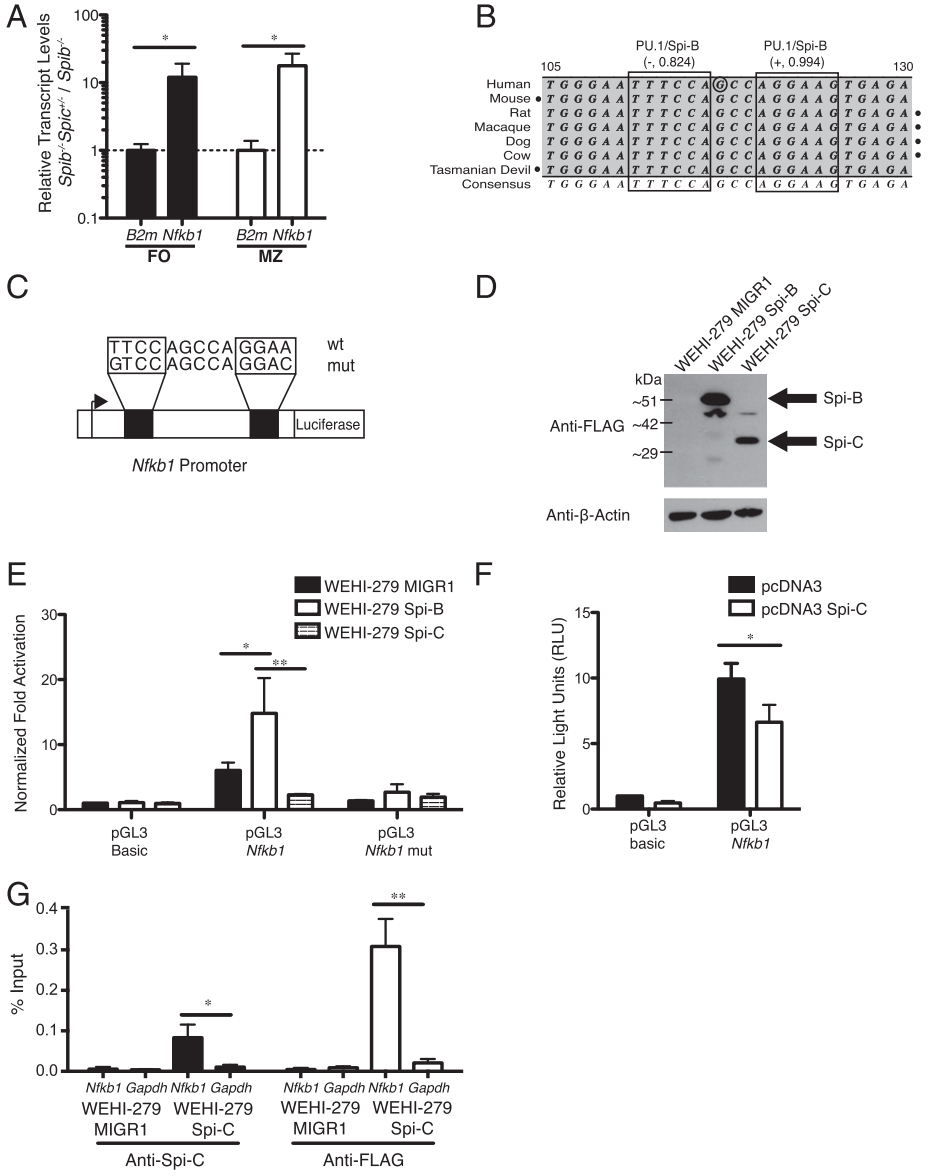

FIGURE 5. Spi-C inhibits activation of the *Nfkb1* promoter by Spi-B. (**A**) Measurement of transcript levels of *Nfkb1* in $Spib^{-/-}Spic^{+/-}$ B cells compared with $Spib^{-/-}$ B cells. Reverse transcription–qPCR analysis was performed on RNA prepared from unstimulated sorted FO and MZ B cells. mRNA transcript levels of genes indicated on the *x*-axis were quantified after normalizing to β2 microglobulin (*B2m*). Data are mean and SD and are a representative of three individual mice. (**B**) Alignment of the of the annotated *Nfkb1* promoter among multiple species, showing nt 105–130 of the conserved 213-bp region. Gray text represents conserved nucleotides, and boxes indicate predicted PU.1/Spi-B binding sites with similarity score and strand location (+/−) listed. Circled nucleotide represents known TSS in the human *Nfkb1* promoter. Dots represent TSS upstream or downstream of the annotated sequence. (**C**) Schematic diagram of luciferase reporter vector. The *Nfkb1* promoter was cloned by PCR and ligated into pGL3-basic. ETS binding sites (wt) were mutated (mut) using site-directed mutagenesis. (**D**) WEHI-279 B cell lymphoma cell lines were generated that overexpress 3XFLAG–Spi-B or Spi-C. Immunoblot analysis demonstrates the overexpression levels of Spi-B or Spi-C in these cell lines. (**E**) Overexpression of Spi-C inhibits activation of the *Nfkb1* promoter. Mutation of the predicted ETS binding sites reduces promoter activity in WEHI-279 MIGR1 and WEHI-279 Spi-B cells. (**F**) Spi-C expression in WEHI-279 Spi-B cells decreases *Nfkb1* activation. WEHI-279 Spi-B cells were cotransfected with a Spi-C expression vector (pcDNA3 Spi-C) along with the luciferase vectors. In (E) and (F), cells were transfected with the plasmids indicated on the *x*-axis. The *y*-axis indicates fold-induction of luciferase activity relative to pGL3-basic. Luciferase activity was normalized by transfection with *Renilla* luciferase expression vector. Data are mean and SEM of three independent experiments. (**G**) Spi-C directly binds to the *Nfkb1* promoter. ChIP analysis was performed on WEHI-279 MIGR1 and WEHI-279 Spi-C cells immunoprecipitated with anti-FLAG or anti–Spi-C Ab. Data show percentage enrichment relative to input for Spi-C interaction with *Nfkb1* and *Gapdh* promoters. Error bars represent SEM from six independent experiments. $*p < 0.05$, $**p < 0.01$, paired Student *t* test.

interacts with the *Nfkb1* promoter, suggesting that it opposes Spi-B–mediated activation of *Nfkb1* transcription in B cells.

Discussion

The purpose of these experiments was to understand how Spi-C contributes to B cell development and function. Spi-C heterozygosity restored many aspects of the $Spib^{-/-}$ phenotype. $Spib^{-/-}Spic^{+/-}$ mice had restored numbers of FO and T2 B cells in their spleens relative to $Spib^{-/-}$ mice. Furthermore, proliferation in response to LPS- and anti-IgM–mediated stimulation was restored in $Spib^{-/-}Spic^{+/-}$ B cells compared with $Spib^{-/-}$ B cells. Investigation of a potential mechanism for the $Spib^{-/-}Spic^{+/-}$ phenotypic rescue revealed that steady-state levels of *Nfkb1* were elevated in sorted FO and MZ B cells from $Spib^{-/-}Spic^{+/-}$

spleens compared with *Spib*$^{-/-}$ spleens. Ectopic expression of Spi-B in B cells resulted in increased *Nfkb1* promoter activity, which was dependent on the ETS binding site. Conversely, overexpression of Spi-C inhibited *Nfkb1* activation by Spi-B. ChIP and ChIP-sequencing analysis demonstrated that both Spi-B and Spi-C are capable of directly binding to the *Nfkb1* promoter. In summary, these results suggest that Spi-C opposes Spi-B in B cell transcriptional regulation.

Intercrosses of *Spib*$^{-/-}$*Spic*$^{+/-}$ mice generated *Spib*$^{-/-}$*Spic*$^{-/-}$ mice at a frequency $< 1\%$ of live births. Similar findings were reported where intercrosses of *Spic*$^{+/-}$ mice generated only 9% *Spic*$^{-/-}$ mice (15). Previous studies demonstrated that injecting embryos with *Spic* small interfering RNA resulted in a reduced rate of blastocyst development (25). It is possible that Spi-B and Spi-C may have overlapping roles in prenatal development; therefore, embryonic death may be occurring at the blastocyst stage in *Spib*$^{-/-}$*Spic*$^{-/-}$ mice. Therefore, the low birth frequency of *Spib*$^{-/-}$*Spic*$^{-/-}$ mice is likely due to reduced embryonic or fetal viability.

Few target genes for Spi-C have been identified in B cells, and Spi-C was reported to function either as an activator or as a repressor of gene transcription. It is possible that altered expression of other unidentified target genes may contribute to the *Spib*$^{-/-}$*Spic*$^{+/-}$ B cell phenotype. Spi-C ectopically expressed in pro-B cells can directly bind and oppose transcription of the *Fcgr2b* gene mediated by PU.1 (13). In contrast, transcription of the gene *Fcer2a*, encoding CD23, was reported to be directly activated by Spi-C in WEHI-279 Spi-C cells (7). Earlier reports showed that Spi-C cooperated with STAT6 to directly induce transcription of IgE under the control of IL-4 (12). In macrophages, Spi-C was reported to transcriptionally activate *Vcam1* expression directly (15). Our data demonstrated that Spi-C directly opposes transcriptional activation of *Nfkb1* by preventing Spi-B, and possibly PU.1, from binding to the *Nfkb1* promoter in B cells. In summary, Spi-C is capable of both activation and repression of its target genes, and it also can transcriptionally regulate target genes by preventing other transcription factors from binding.

Previous studies demonstrated that the transcription factors PU.1 and Spi-B are required to maintain proper levels of *Nfkb1* in B cells (23). Spi-B directly binds to the *Nfkb1* promoter and activates transcription. In contrast, Spi-C directly binds to the *Nfkb1* promoter, but it does not activate transcription. Therefore, decreased Spi-C expression may reduce its occupancy of the *Nkfb1* promoter in *Spib*$^{-/-}$*Spic*$^{+/-}$ B cells, permitting increased activation of *Nfkb1* by PU.1. Elevated *Nfkb1* transcript levels in *Spib*$^{-/-}$*Spic*$^{+/-}$ B cells compared with *Spib*$^{-/-}$ B cells suggest that Spi-C and Spi-B oppose each other to regulate appropriate *Nfkb1* levels. *Spib*$^{-/-}$ and *Nfkb1*$^{-/-}$ B cells proliferate similarly to LPS and anti-IgM. LPS-stimulated *Nfkb1*$^{-/-}$ B cells fail to proliferate, and anti-IgM stimulation results in reduced proliferation (22). Overall, elevated *Nfkb1* expression in *Spib*$^{-/-}$*Spic*$^{+/-}$ B cells compared with *Spib*$^{-/-}$ B cells may sufficiently explain the rescue in proliferation.

Spib$^{-/-}$*Spic*$^{+/-}$ mice have restored FO and T2 B cell numbers compared with *Spib*$^{-/-}$ mice, indicating that Spi-B and Spi-C regulate peripheral B cell differentiation. FO and T2 cell differentiation both require NF-κB signaling and BCR signaling. Transitioning from a T1 to a T2 B cell requires noncanonical NF-κB signals and basal BCR signals, and maturation of a T2 B cell to an FO B cell requires canonical NF-κB signals and strong BCR signaling (1). *Nfkb1*$^{-/-}$*Nfkb2*$^{-/-}$ mice have a developmental block at the T2 stage and fail to generate any mature B cells (26). Therefore, elevated *Nfkb1* expression in developing *Spib*$^{-/-}$*Spic*$^{+/-}$ mice could be sufficient to explain the restored FO B cell population. It is also conceivable that Spi-C may be a negative regulator of c-Rel expression, because PU.1 and Spi-B were reported to directly activate *Rel* transcription (27). Alternatively, it is possible that FO and T2 B cells in *Spib*$^{-/-}$*Spic*$^{+/-}$ mice have a longer lifespan than in *Spib*$^{-/-}$ B cells, which could contribute to restoration of FO and T2 B cells. *Spib*$^{-/-}$ B cells have impaired BCR signaling and, thus, proliferate poorly in response to anti-IgM stimulation (4, 5). Transgenic Spi-C expression in B cells results in reduced transcript levels of the BCR signaling genes *Btk* and *Blnk* in FO B cells (14). Restored proliferative responses to anti-IgM in *Spib*$^{-/-}$*Spic*$^{+/-}$ B cells compared with *Spib*$^{-/-}$ B cells suggest that BCR signaling is possibly restored as a result of reduced Spi-C expression. Because WT, *Spib*$^{-/-}$, and *Spib*$^{-/-}$*Spic*$^{+/-}$ B cells are capable of phosphorylating Syk at equivalent levels following anti-IgM stimulation, the rescue in BCR signaling is likely downstream of Syk. Therefore, rescued FO and T2 B cells in *Spib*$^{-/-}$*Spic*$^{+/-}$ spleens might be caused by a combination of restored NF-κB and BCR signaling.

It is possible that aspects of the B cell phenotype of *Spib*$^{-/-}$*Spic*$^{+/-}$ mice are not cell intrinsic. However, evidence was provided for a cell-intrinsic effect of Spi-C on B cell proliferation using the Eμ–Spi-C transgenic mouse. In this mouse model, the Spi-C transgene is under the control of a lymphocyte-specific Eμ intronic enhancer. We found that crossing this transgenic mouse to *Spib*$^{-/-}$*Spic*$^{+/-}$ mice (Eμ–Spi-C *Spib*$^{-/-}$*Spic*$^{+/-}$) resulted in a reduction in proliferation from isolated B cells, suggesting that Spi-C has a cell-intrinsic effect on B cell function. Furthermore, overexpression of Spi-C in Eμ–Spi-C *Spib*$^{-/-}$*Spic*$^{+/-}$ mice reduced the number of FO and MZ B cells, suggesting a cell-intrinsic role for Spi-C in B cell development.

In summary, our results demonstrate a novel mechanism for Spi-C as a negative regulator of B cell development and function. Understanding transcriptional regulation in B cells has human health implications, because dysfunctional B cell development can lead to leukemia of the B cell lineage (8, 19). Furthermore, Ab formation in B cells is transcriptionally regulated, so understanding the potential activators and repressors of this process can improve interventions for vaccine development. Further analysis on mice lacking Spi-B and reduced Spi-C can provide additional insight into other genes involved in B cell development, function, and disease.

Acknowledgments

We thank Dr. Kenneth M. Murphy (Washington University School of Medicine) for the gift of *Spic*$^{-/-}$ mice. We acknowledge the London Regional Genomics core facility for assisting with DNA sequencing and Kristin Chadwick from the London Regional Flow Cytometry for performing cell sorting.

Disclosures

The authors have no financial conflicts of interest.

References

1. Pillai, S., and A. Cariappa. 2009. The follicular versus marginal zone B lymphocyte cell fate decision. *Nat. Rev. Immunol.* 9: 767–777.
2. Scott, E. W., M. C. Simon, J. Anastasi, and H. Singh. 1994. Requirement of transcription factor PU.1 in the development of multiple hematopoietic lineages. *Science* 265: 1573–1577.
3. Houston, I. B., M. B. Kamath, B. L. Schweitzer, T. M. Chlon, and R. P. DeKoter. 2007. Reduction in PU.1 activity results in a block to B-cell development, abnormal myeloid proliferation, and neonatal lethality. *Exp. Hematol.* 35: 1056–1068.
4. Su, G. H., H. M. Chen, N. Muthusamy, L. A. Garrett-Sinha, D. Baunoch, D. G. Tenen, and M. C. Simon. 1997. Defective B cell receptor-mediated responses in mice lacking the Ets protein, Spi-B. *EMBO J.* 16: 7118–7129.
5. Garrett-Sinha, L. A., G. H. Su, S. Rao, S. Kabak, Z. Hao, M. R. Clark, and M. C. Simon. 1999. PU.1 and Spi-B are required for normal B cell receptor-mediated signal transduction. *Immunity* 10: 399–408.
6. Ray-Gallet, D., C. Mao, A. Tavitian, and F. Moreau-Gachelin. 1995. DNA binding specificities of Spi-1/PU.1 and Spi-B transcription factors and identification of a Spi-1/Spi-B binding site in the c-fes/c-fps promoter. *Oncogene* 11: 303–313.

7. DeKoter, R. P., M. Geadah, S. Khoosal, L. S. Xu, G. Thillainadesan, J. Torchia, S. S. Chin, and L. A. Garrett-Sinha. 2010. Regulation of follicular B cell differentiation by the related E26 transformation-specific transcription factors PU.1, Spi-B, and Spi-C. *J. Immunol.* 185: 7374–7384.
8. Sokalski, K. M., S. K. Li, I. Welch, H. A. Cadieux-Pitre, M. R. Gruca, and R. P. DeKoter. 2011. Deletion of genes encoding PU.1 and Spi-B in B cells impairs differentiation and induces pre-B cell acute lymphoblastic leukemia. *Blood* 118: 2801–2808.
9. Rothenberg, E. V. 2014. Transcriptional control of early T and B cell developmental choices. *Annu. Rev. Immunol.* 32: 283–321.
10. Bemark, M., A. Mårtensson, D. Liberg, and T. Leanderson. 1999. Spi-C, a novel Ets protein that is temporally regulated during B lymphocyte development. *J. Biol. Chem.* 274: 10259–10267.
11. Carlsson, R., C. Persson, and T. Leanderson. 2003. SPI-C, a PU-box binding ETS protein expressed temporarily during B-cell development and in macrophages, contains an acidic transactivation domain located to the N-terminus. *Mol. Immunol.* 39: 1035–1043.
12. Carlsson, R., K. Thorell, D. Liberg, and T. Leanderson. 2006. SPI-C and STAT6 can cooperate to stimulate IgE germline transcription. *Biochem. Biophys. Res. Commun.* 344: 1155–1160.
13. Schweitzer, B. L., K. J. Huang, M. B. Kamath, A. V. Emelyanov, B. K. Birshtein, and R. P. DeKoter. 2006. Spi-C has opposing effects to PU.1 on gene expression in progenitor B cells. *J. Immunol.* 177: 2195–2207.
14. Zhu, X., B. L. Schweitzer, E. J. Romer, C. E. Sulentic, and R. P. DeKoter. 2008. Transgenic expression of Spi-C impairs B-cell development and function by affecting genes associated with BCR signaling. *Eur. J. Immunol.* 38: 2587–2599.
15. Kohyama, M., W. Ise, B. T. Edelson, P. R. Wilker, K. Hildner, C. Mejia, W. A. Frazier, T. L. Murphy, and K. M. Murphy. 2009. Role for Spi-C in the development of red pulp macrophages and splenic iron homeostasis. *Nature* 457: 318–321.
16. Haldar, M., M. Kohyama, A. Y. So, W. Kc, X. Wu, C. G. Briseño, A. T. Satpathy, N. M. Kretzer, H. Arase, N. S. Rajasekaran, et al. 2014. Heme-mediated SPI-C induction promotes monocyte differentiation into iron-recycling macrophages. *Cell* 156: 1223–1234.
17. Itoh-Nakadai, A., R. Hikota, A. Muto, K. Kometani, M. Watanabe-Matsui, Y. Sato, M. Kobayashi, A. Nakamura, Y. Miura, Y. Yano, et al. 2014. The transcription repressors Bach2 and Bach1 promote B cell development by repressing the myeloid program. *Nat. Immunol.* 15: 1171–1180.
18. Pfaffl, M. W., G. W. Horgan, and L. Dempfle. 2002. Relative expression software tool (REST) for group-wise comparison and statistical analysis of relative expression results in real-time PCR. *Nucleic Acids Res.* 30: e36.
19. Xu, L. S., K. M. Sokalski, K. Hotke, D. A. Christie, O. Zarnett, J. Piskorz, G. Thillainadesan, J. Torchia, and R. P. DeKoter. 2012. Regulation of B cell linker protein transcription by PU.1 and Spi-B in murine B cell acute lymphoblastic leukemia. *J. Immunol.* 189: 3347–3354.
20. Hardy, R. R., C. E. Carmack, S. A. Shinton, J. D. Kemp, and K. Hayakawa. 1991. Resolution and characterization of pro-B and pre-pro-B cell stages in normal mouse bone marrow. *J. Exp. Med.* 173: 1213–1225.
21. Pone, E. J., H. Zan, J. Zhang, A. Al-Qahtani, Z. Xu, and P. Casali. 2010. Toll-like receptors and B-cell receptors synergize to induce immunoglobulin class-switch DNA recombination: relevance to microbial antibody responses. *Crit. Rev. Immunol.* 30: 1–29.
22. Sha, W. C., H. C. Liou, E. I. Tuomanen, and D. Baltimore. 1995. Targeted disruption of the p50 subunit of NF-kappa B leads to multifocal defects in immune responses. *Cell* 80: 321–330.
23. Li, S. K. H., A. K. Abbas, L. A. Solomon, G. M. N. Groux, and R. P. DeKoter. 2015. Nfkb1 activation by the ETS transcription factors PU.1 and Spi-B promotes toll-like receptor-mediated splenic B cell proliferation. *Mol. Cell. Biol.* DOI: 10.1128/MCB.00117-15.
24. Cogswell, P. C., R. I. Scheinman, and A. S. Baldwin. 1993. Promoter of the human NF-kappa B p50/p105 gene. Regulation by NF-kappa B subunits and by c-REL. *J. Immunol.* 150: 2794–2804.
25. Kageyama, S., H. Liu, M. Nagata, and F. Aoki. 2006. The role of ETS transcription factors in transcription and development of mouse preimplantation embryos. *Biochem. Biophys. Res. Commun.* 344: 675–679.
26. Claudio, E., K. Brown, S. Park, H. Wang, and U. Siebenlist. 2002. BAFF-induced NEMO-independent processing of NF-kappa B2 in maturing B cells. *Nat. Immunol.* 3: 958–965.
27. Hu, C. J., S. Rao, D. L. Ramirez-Bergeron, L. A. Garrett-Sinha, S. Gerondakis, M. R. Clark, and M. C. Simon. 2001. PU.1/Spi-B regulation of c-rel is essential for mature B cell survival. *Immunity* 15: 545–555.